Comparison between Quantum Confinement Effects of Quantum Wires and Dots

Jingbo Li and Lin-Wang Wang*

Computational Research Division, Lawrence Berkeley National Laboratory, Berkeley, California 94720

Received March 24, 2004. Revised Manuscript Received August 4, 2004

Dimensionality is an important governing factor in the electronic structures of semiconductor nanocrystals. The quantum confinement energies in one-dimensional quantum wires and zero-dimensional quantum dots are quite different. Using large-scale first-principle calculations, we have systematically studied the electronic structures of semiconductor (including group IV, III−V, and II−VI materials) surface-passivated quantum wires and dots. We have found that the band-gap energies of quantum wires and dots have the same scaling with diameter for a given material. The ratios of band-gap increases between quantum wires and dots are material-dependent, and for most direct band-gap materials, this ratio is very close to 0.586, as predicted by simple effective-mass approximation. We also have found a highly linear polarization of photoluminescence in quantum wires. The degree of polarization decreases with the increasing temperature and quantum wire size.

1. Introduction

Semiconductor nanocrystals, such as quantum dots (QDs)[1] and quantum wires (QWs),[2] are of intense scientific and technological interest. Their electronic structures can be tailored by size and shape, leading to many new applications, including lasers,[3] biological cell labeling,[4] and solar cells.[5] Previously, the study of QWs attracted less interest than QDs because of the technical difficulties in synthesizing them. Recently, however, high-quality semiconductor QWs have been fabricated by a solution−liquid−solid approach in wet chemistry.[4−9] The diameter of the QWs synthesized by this method is small enough to show strong quantum confinement effects, similar to those found in colloidal QDs. Given the recent advances in QWs, one obvious task is to compare the quantum confinement effects in QWs and QDs. This gives us a way to study the effects of dimensionality[9] in quantum confinement systems.

According to an overly simplified particle-in-a-box effective-mass model,[10−12] the band-gap increases of QDs and QWs from the bulk value are $\Delta E_g = (2\hbar^2\zeta^2)/(m^*d^2)$, where $1/(m^*) = 1/(m_e^*) + 1/(m_h^*)$ (m_e^* and m_h^* are electron and hole effective-masses, respectively) and d is the diameter. For spherical QDs, $\zeta = \pi$ is the zero point of the spherical Bessel function, whereas for cylindrical QWs, $\zeta = 2.4048$ is the zero point of the cylindrical Bessel function. Thus, the ratio of band-gap increases between QWs and QDs should be $\Delta E_g^{wire}/\Delta E_g^{dot} = 0.586$. There are two questions about this simple effective-mass model: (1) Does the ΔE_g follow the $1/d^2$ scaling? (If not, do the QW and QD ΔE_g have the same scaling?) (2) Is the real ratio of $\Delta E_g^{wire}/\Delta E_g^{dot}$ close to 0.586?

These questions were addressed to some extent through earlier experiments on such systems as InP and CdSe,[6−8] where a "rule of thumb" 0.6 ratio between quantum wire and quantum dot confinements was observed. Here, we address the same questions using ab initio calculations for many more materials: Si, InP, InAs, GaAs, CdSe, CdS, and CdTe. Unlike the experiments, where the exact diameters of QDs and QWs always had some uncertainties, these uncertainties do not exist in our ab initio calculations.

To do ab initio calculations for thousand-atom colloidal systems, we use the recently developed charge-patching method. This method has been applied successfully to calculate the electronic structure of an unconventional semiconductor alloy with a supercell containing 4096 atoms[13−15] and of group IV−IV, III−V, and II−VI 1000-atom semiconductor QDs.[16] Prior to the charge-patching method, the empirical pseudopotential method (EPM) was used to calculate the electronic structure of semiconductor nanocrystals.[17,18] Compared

* Corresponding author. E-mail: lwwang@lbl.gov.

(1) Alivisatos, A. P. *Science* **1996**, *271*, 933.
(2) Xia, Y.; et al. *Adv. Mater.* **2003**, *15*, 353.
(3) Huang, M.; Mao, S.; Feick, H.; Yan, H.; Wu, Y.; Kind, H.; Weber, E.; Russo, R.; Yang, P. *Science* **2001**, *292*, 1897.
(4) Bruchez, M.; Moronne, M.; Gin, P.; Weiss, S.; Alivisatos, A. P. *Science* **1998**, *281*, 2013.
(5) Huynh, W. U.; Dittmer, J. J.; Alivisatos, A. P. *Science* **2002**, *295*, 2425.
(6) Yu, H.; Li, J.; Loomis, R. A.; Gibbons, P. C.; Wang, L. W.; Buhro, W. E., *J. Am. Chem. Soc.* **2003**, *125*, 16168.
(7) Yu, H.; Li, J.; Loomis, R. A.; Wang, L. W.; Buhro, W. E. *Nature Mater.* **2003**, *2*, 517.
(8) Duan, X.; Lieber, C. M. *Adv. Mater.* **2000**, *12*, 298.
(9) Kan, S.; Mokari, T.; Rothenberg, E.; Banin, U. *Nature Mater.* **2003**, *2*, 155.
(10) Zheng, W. H.; Xia, J. B.; Cheah, K. W. *J. Phys.: C* **1997**, *9*, 5105.
(11) Li, J.; Xia, J. B. *Phys. Rev. B* **2000**, *61*, 15880.
(12) Xia, J. B.; Li, J. *Phys. Rev. B* **1999**, *60*, 11540.
(13) Wang, L. W. *Phys. Rev. Lett.* **2002**, *88*, 256402.
(14) Li, J.; Wang, L. W. *Phys. Rev. B* **2003**, *67*, 205319.
(15) Li, J.; Wang, L. W. *Phys. Rev. B* **2003**, *67*, 033102.
(16) Wang, L. W.; Li, J. *Phys. Rev. B*, **2004**, 69, 153302.
(17) Wang, L. W.; Zunger, A. *Phys. Rev. B* **1996**, *53*, 9579.

10.1021/cm0494958 CCC: $27.50
Published on Web 09/23/2004

to the EPM method, the charge-patching method has the following advantages: (1) There are no fitting uncertainties, such as those found in the EPM method. Thus, there is no need for a fitting procedure. Using the charge-patching method, the local density approximation (LDA)-quality charge density of a large nanosystem can be calculated directly without having to do a self-consistent LDA calculation for the large system. (2) The surface passivation of a colloidal nanosystem is straightforward and physical. In EPM, it takes a long time to fit a surface passivation for a given material. Although the use of the charge-patching method in earlier tests had proven highly effective, this method is relatively new, especially in its application to colloidal nanocrystals. Thus, in addition to our main task, comparing the quantum confinement effects in QWs and QDs, we will also check the accuracy of the charge-patching method relative to direct LDA calculations, especially in the case of QWs.

2. Method

The calculation scheme for the charge-patching method is as follows. First, we use pseudo-hydrogen atoms (with fractional nuclei charges and numbers of electrons) on the surface of QWs, which provides an ideal passivation to pair the electron in the dangling bonds. Second, we generate the ab initio quality electron charge density $\rho_{\text{patch}}(r)$ using charge motifs generated from prototype systems with similar atomic environments. Third, via the solution of Poisson's equation, we use the standard LDA formula to calculate the total LDA potential $V(r)$. Then the single particle Schrödinger's (or Kohn−Sham's) equation $[-1/2\nabla^2 + V(r)]\Psi_i = \epsilon_i\Psi_i$ can be solved using the linear scaling folded spectrum method (FSM) for the band edge states.[19] The FSM searches for the minimum of $\langle Y_i|(H - E_{\text{ref}})^2|\Psi_i\rangle$, where E_{ref} is a reference energy placed inside the band gap. The details of this entire procedure are published in Wang and Li.[16]

We use ideal crystal structures and bulk lattice constants for the quantum dots and wires. This is consistent with the experimental finding[20−22] that the lattice constant for a colloidal quantum dot is within 0.1−0.2% of its bulk value. The corresponding uncertainty in the eigen energies is on the order of 10 meV. A recent LDA total-energy atomic relaxation calculation[23] also showed that, even for an extremely small quantum dot containing only 60 atoms, the interior of the dot retains its bulk crystal structure. At the surface, we use H atoms to passivate the Si dangling bonds and artificial fractionally charged pseudo-H atoms to passivate the cations and anions of the III−V and II−VI semiconductors. More specifically, the fractional Z charges used to passivate the II, III, V, and VI surface atoms are 1.5, 1.25, 0.75, and 0.5, respectively. These pseudo-H atoms are placed at the ideal orientations of the surface dangling bonds, but with a surface atom-H bond length equal to half of the bulk bond length. Note that, although these pseudo-H atoms are artificial, they capture the essence of any good surface passivation by organic ligand molecules. In addition, as long as the dangling bonds are filled and their energies are moved away from the band gap, our band gap results do not depend on the details of the surface passivation. In the charge-patching method, atomic charge motifs for pseudo-H atoms belonging to different passivating groups (e.g., AH and AH2, where A is the passivated surface atom) are generated from flat surface calculations.

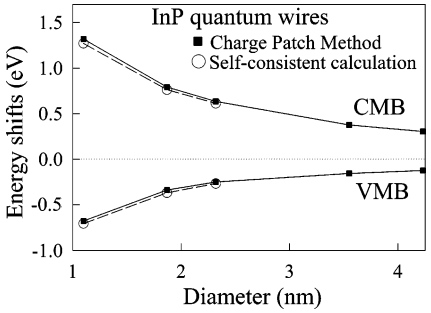

Figure 1. CBM and VBM band energy shifts of InP QWs from the bulk values. The full-squares correspond to the results of the charge-patching method. The LDA self-consistent calculations are shown as open dots.

Table 1. Zinc-Blend Lattice *a* (in Å) and Kinetic Energy Cutoff (in Ry) for the Plane-Wave Basis Set Used in the Calculations

	Si	GaAs	InAs	InP	CdSe	CdS	CdTe
a (Å)	5.43	5.65	6.06	5.87	6.08	5.82	6.48
E_{cut} (Ry)	25.0	25.0	25.0	25.0	35.0	25.0	25.0

We have studied Si, GaAs, InAs, InP, CdSe, CdS, and CdTe QWs in [111] growth directions (also called c-axis or z-direction herein). In this work, we use zinc-blend crystal structures for all materials. We use the experimental bulk lattice constants shown in Table 1. The effective diameter of QWs is defined in terms of the number of atoms N_{wire} (not counting the surface pseudo-H atoms) in a wire (with one periodicity along [111] c-axis, i.e., six atomic monolayers) as $d = a((\sqrt{3}/6\pi)N_{\text{wire}})^{1/2}$, where a is the bulk lattice constant. We use plane-wave basis sets and norm-conserving pseudopotentials in our calculations. The kinetic energy cutoff for the plane-wave basis set is listed in Table 1. We have found our calculated bulk band structures are in excellent agreement with all electron linearized augmented plane wave (LAPW) method results.[24] The real space grid for the largest quantum wire is 320 × 320 × 64.

3. Results and Discussion

First, we test the relative accuracy of the charge-patching method by comparing its results with the direct self-consistent LDA calculated results. We use InP as our test case, although similar results are found for other systems. Figure 1 plots the energy shifts (from their bulk values) of the conduction band minimum (CBM) and valence band maximum (VBM) states of InP QWs. The largest errors (48 meV in CBM and 29 meV in VBM) are found in the QWs with a diameter of 1.10 nm. After QW sizes increase beyond 2 nm, the single particle eigen energies cause an error within the 20 meV range, compared to the direct LDA calculations. The errors of band gap ΔE_g shown in Table 2 are even smaller. The 1.10 nm QWs have 19 meV error. The QWs larger than 2 nm have typical errors of just ≤5 meV. Compared to the band gap, the slightly larger errors in CBM and VBM might be the consequences of different potential alignments between the charge-patching method and the direct LDA method. For the bulk InP, which can be thought of as very large size

(18) Li, J.; Wang, L. W. *Nano Lett.* **2003**, *3*, 101; *Nano Lett.* **2003**, *3*, 1357; *Nano Lett.* **2004**, *4*, 29.
(19) Wang, L. W.; Zunger, A. *J. Phys. Chem. B* **1998**, *102*, 6449.
(20) Littau, K. A.; Szajoski, P. J.; Muller, A. J.; Kortan, A. R.; Brus, L. E. *J. Phys. Chem.* **1993**, *97*, 1224.
(21) Takagi, H.; Ogawa, H.; Yamazaki, Y.; Ishizaki, A.; Nakagiri, T. *Appl. Phys. Lett.* **1990**, *56*, 2379.
(22) Zhang, J.; Wang, X. Y.; Xiao, M.; Qu, L.; Peng, X. *Appl. Phys. Lett.* **2002**, *81*, 2076.
(23) Puzder, A.; Williamson, A. J.; Gygi, F.; Galli, G. *Phys. Rev. Lett.* **2004**, *92*, 217401.
(24) Wei, S. H.; Zunger, A. *Phys. Rev. B* **1999**, *60*, 5404.
(25) Wang, J. F.; Gudiksen, M. S.; Duan, X.; Cui, Y.; Lieber, C. M. *Science* **2001**, *293*, 1455.
(26) Li, X. Z.; Xia, J. B. *Phys. Rev. B* **2002**, *66*, 115316.

Table 2. Accuracy of the Charge-Patching Method Compared to Direct Self-Consistent LDA Calculations[a]

system	$\Delta\rho$ (%)	ΔE_g (meV)
InP (bulk)	0.067	3×10^{-4}
InP(100)	0.32	18
InP(111)	0.39	22
InP(110)	0.33	15
$d = 1.10$ nm	0.97	19
$d = 1.87$ nm	0.72	1
$d = 2.32$ nm	0.62	3

[a] The band gap errors for the eigen states of other materials are similar to the band gap errors shown here. InP(100), -(111), and -(110) denote three flat surface slab calculations, while the last three rows show three quantum wires with different diameters.

QWs (infinite diameter), it has a 3×10^{-4} meV error in the gap. The accuracy of the patched charge density $\rho_{patch}(r)$ can be measured by comparing it to the directly calculated self-consistent LDA charge density $\rho_{LDA}(r)$ as follows: $\Delta\rho = \int\{|\rho_{patch}(r) - \rho_{LDA}(r)|\, d^3r\}/\{\int\rho_{LDA}(r)\, d^3r\}$. The results are shown in Table 2 for different systems. Overall, we get a charge density error of less than 1%, similar to what we found for semiconductor QDs.[16]

The above tests establish the accuracy of the charge-patching method when compared with the direct ab initio LDA method. This, however, does not address the problems in the LDA method itself. It is well-known that the LDA gives smaller band gaps when compared with the experimental results. In addition, because of the under estimate of the band gap, the LDA also gives smaller conduction band effective masses. While the small band gap might not be a problem in our study, since we are only concerned with the change of the band gap due to quantum confinement, the small effective mass does tend to overestimate the quantum confinement effects. As a result, our LDA band gap quantum confinement results listed below are somewhat larger than the experimentally measured values and the EPM calculated results. That is one of the reasons we focus here on the comparison between QW and QD. Since LDA error affects the QW and QD quantum confinements in the same way for a given material, we believe that the ratio of their quantum confinements is depicted accurately by LDA. This is confirmed below by comparing the current LDA results with previous EPM results.

Next, we use the charge-patching method to study the electronic states of various QWs. In Figure 2, we show the contour plots of charge density distribution for the CBM state and VBM state of a 4.23 nm diameter InP QW. The wave functions of both CBM and VBM states are distributed mostly in the interior of the wire rather than at the surface. The envelope functions of both CBM and VBM states are σ-type (s-like in the xy plane). The electronic band structure of InP QWs with a diameter of 4.23 nm is plotted in Figure 3a. In the conduction band, the lowest energy state is σ_c, and the next higher energy state is π_c (p-like envelope function in the xy plane) with double degeneracy. The subscript c stands for the conduction band. In the valence band, the highest energy state is σ_z. Here, the subscript z indicates the Bloch part of the wave function having a p_z character. The next lower energy state is π_z with a double degeneracy. Lower than that, the states are π_{xy} with a double degeneracy. Here, the subscribe xy indicates the p_{xy} character of the Bloch part of the wave function.

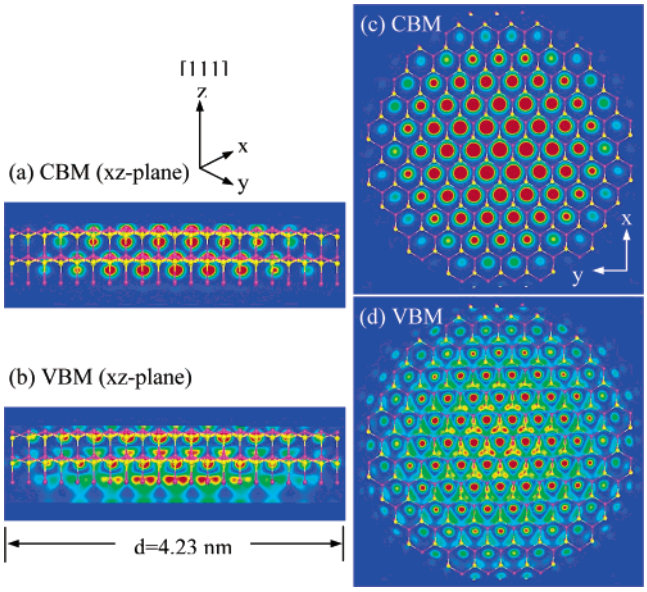

Figure 2. Contour plot of charge density distribution of (a) CBM and (b) VBM states of InP QWs on an xz-plane cross section and (c) CBM and (d) VBM on an xy-plane cross section. Magenta dots represent In-atoms; yellow dots represent P-atoms. Due to a special setting in the plotting program, the lowest layer of the P-atoms is not shown in (a) and (b), and the surface pseudo-H atoms are not plotted in this figure. Red, yellow, green, and blue colors indicate electron density from higher to lower.

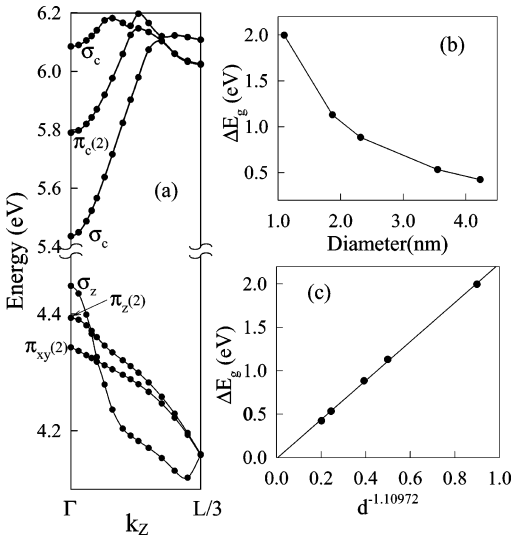

Figure 3. (a) Electronic band structure of InP QWs with a diameter of 4.23 nm. The numbers in parentheses indicate the degeneracy of the states. (b) The change of the band gap, ΔE_g, as a function of the diameter d of the InP QWs. (c) The linear least-squares fitting to ΔE_g for InP QWs.

The band gap change ΔE_g as a function of the QW diameter is plotted in Figure 3b. We fit ΔE_g with diameter d using the expression $\Delta E_g = \{\beta/d^{\alpha}\}$. We get $\alpha = 1.10972$ for InP QWs. The quality of the fitting is shown in Figure 3c. This α value is far removed from the simple effective-mass value of $\alpha = 2$.

We have done the same fitting for the calculated QD band gaps. The fitted results of α and β are listed in Table 3 for all the systems we have calculated. By comparing the QD and QW values, we can observe the

Table 3. α and β for the β/d^{α} Fit of the ΔE_g for Different Materials[a]

	Si	GaAs	InAs	InP	CdSe	CdS	CdTe
β_{dot}	3.81	3.88	4.41	3.90	3.84	3.35	4.40
α_{dot}	1.60	1.01	1.01	1.10	1.18	1.22	1.28
β_{wire}	1.53	2.18	2.58	2.21	2.19	1.97	2.20
α_{wire}	1.53	0.97	0.98	1.11	1.20	1.30	1.18
β'_{wire}	1.55	2.15	2.62	2.21	2.20	1.91	2.18
$\beta'_{wire}/\beta_{dot}$	0.408	0.554	0.595	0.566	0.572	0.571	0.496

[a] The unit of β is eV × (nm)$^{\alpha}$. The QDs parameters of β_{dot} and α_{dot} are reported in Wang and Li.[16] We list these here for comparison with those of QWs. Using α_{dot} to fit the ΔE_g of QWs, we get β'_{wire}.

following: (1) The difference for α between QD and QW for the same material is very small. Typically, these differences are within 4%, except in the case of CdS and CdTe, where the difference is ∼6−8%. (2) For these small differences, there is no systematic trend. For example, one cannot say that the α value from QW is larger or smaller than that from QD. (3) Given the small differences and the lack of a trend, one can assume that the difference for α between QW and QD is probably due to fluctuation of the fitting; thus, they can be set as the same. Note that the differences for α between different materials are more significant. Roughly, the IV−IV material of Si has $\alpha \approx 1.6$, while the III−V materials have $\alpha \approx 1.0$, and the II−V materials have $\alpha \approx 1.2$.

By assuming α_{dot} to be the same as α_{wire}, we can use α_{dot} to fit the ΔE_g of the QWs. That gives us a new β'_{wire}, which is also listed in Table 3. As a result, the $\{\Delta E_g^{wire}(d)\}/\{\Delta E_g^{dot}(d)\}$ ratio will just be the ratio of $\{\beta'_{wire}\}/\{\beta_{dot}\}$. We have found this ratio to range from 0.408 (for Si) to 0.595 (for InAs). Except for Si and CdTe, these ratios are very close to the simple effective mass results of 0.586. The small ratio for Si is probably due to the indirect nature of its band gap, where its effective mass near the X point is highly asymmetric. For InP and CdSe, our LDA ratios of 0.566 and 0.572 are very close to their EPM values of 0.570 and 0.561, respectively.[7,6] This indicates that, despite the LDA errors, the ratios between QW and QD are captured accurately by its results. Notice that these ratios are calculated before the electron and hole Coulomb interactions are included in the single particle band gap to get the exciton energies. If the Coulomb interaction energy is added to the QD results alone, then these ratios will be larger (in the range of 0.70). However, since there are some uncertainties in how to calculate the Coulomb interactions in the QWs, in this case we have decided not to include the Coulomb energy in both QDs and QWs.

Finally, to highlight the difference between the QW and QD electronic structures, we have calculated the photoluminescence (PL) polarization. The QW PL is usually highly polarized along the *z*-direction. This can be used as an experimental indicator to distinguish the QWs from the QDs. It also opens doors to new device applications such as polarization-sensitive nanoscale photodetectors, integrated photonic circuits, optical switches, and interconnects.[25] However, the polarization might be temperature sensitive, especially for large QWs. To get this temperature dependence, we have

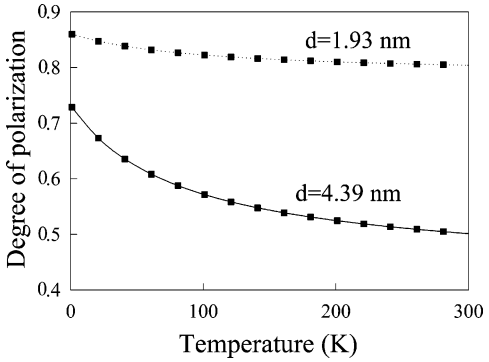

Figure 4. Degree of linear polarization as a function of temperature for CdSe QWs with diameters of 1.93 and 4.39 nm.

calculated 40 conduction band states and 40 valence band states for 100 k_z points for each of the two CdSe QWs with $d = 1.93$ and 4.39 nm, respectively. The optical transition matrix elements between these 40 states are calculated, and the Boltzmann distribution is used to occupy the states. The PL polarizations along *z* and *xy* directions are calculated for different temperatures. The resulting linear polarization defined as $P = (I_{||} - I_{\perp})/(I_{||} + I_{\perp})$[26] is shown in Figure 4. We find that for the small QWs, the polarization is always high and almost independent of the temperature, while for the large QWs, the polarization is significantly reduced at room temperature from the zero temperature value.

4. Conclusions

We have performed ab initio charge-patching calculations for large-scale semiconductor QWs and confirmed the accuracy of these calculations in 1000-atom QW applications. The present method is applied to all the semiconductor systems without any fitting parameters. The errors of eigen energies compared with self-consistent LDA calculations are in the order of 20 meV. Both the calculated QW and QD band gaps can be described by the formula $\Delta E_g = \{\beta/d^{\alpha}\}$ with material-dependent parameters α and β. We find that for a given material, QWs and QDs have the same $1/d^{\alpha}$ scaling. However, α is different from the simple effective-mass value of 2. The ratios of QW and QD band gaps for most direct band gap materials are very close to 0.586, as predicted by effective-mass approximation. Finally, we have studied the linear polarization of PL in QWs. The degree of polarization decreases with increasing temperature and size. However, for small QWs, the degree of polarization is high and almost independent of temperature.

Acknowledgment. The authors thank Prof. William E. Buhro, of Washington University, for fruitful discussions. This work is supported by the U.S. Department of Energy, under Contract No. DE-AC03-76SF00098. This research used the resources of the National Energy Research Scientific Computing Center at Lawrence Berkeley National Laboratory.

CM0494958